

Evidence of ultra-low-k dielectric material degradation and nanostructure alteration of the Cu/ultra-low-k interconnects in time-dependent dielectric breakdown failure

Jeffrey C. K. Lam,^{1,2} Maggie Y. M. Huang,^{1,a)} Tsu Hau Ng,¹ Mohammed Khalid Bin Dawood,¹ Fan Zhang,¹ Anyan Du,¹ Handong Sun,² Zexiang Shen,² and Zhihong Mai¹
¹GLOBALFOUNDRIES Singapore Pte Ltd, Woodlands Industrial Park D, Street 2, Singapore 738406
²Division of Physics and Applied Physics, School of Physical and Mathematical Sciences, Nanyang Technological University, Singapore 637371

(Received 25 October 2012; accepted 3 January 2013; published online 16 January 2013)

Ultra-low-k time-dependent dielectric breakdown (TDDB) is one of the most important reliability issues in Cu/low-k technology development due to its weaker intrinsic breakdown strength compared to SiO₂ dielectrics. With continuous technology scaling, this problem is further exacerbated for Cu/ultra-low-k interconnects. In this letter, the TDDB degradation behavior of ultra-low-k dielectric in Cu/ultra-low-k interconnects will be investigated by a method consisting of a combination of Raman with Fourier transform infrared vibrational microscopes. In TDDB tests on Cu/low-k interconnect, it was found that intrinsic degradation of the ultra-low-k dielectric would first occur under electrical field stress. Upon further electrical field stress, the ultra-low-k dielectric degradation would be accelerated due to Ta ions migration from the Ta/TaN barrier bi-layer into the ultra-low-k dielectrics. In addition, no out-diffusion of Cu ions was observed in our investigation on Cu/Ta/TaN/SiCOH structures. © 2013 American Institute of Physics. [<http://dx.doi.org/10.1063/1.4776735>]

Cu and low-k or ultra-low-k dielectrics have been widely used as interconnects in current leading edge semiconductor technologies. Damascene and dual-damascene processes were applied to form IC interconnects to achieve significant reduction in RC delays. However, due to the weak strength of ultra-low-k dielectric materials, inter-metal-dielectric (IMD) reliability becomes a big concern.¹ Time-dependent dielectric breakdown (TDDB) is one of the most common IMD reliability tests.² A significant amount of studies on electric field dependence of the TDDB time to failure (TTF) have been conducted. The TDDB E and square root E models have been proposed and are currently being used by most researchers for fitting TDDB plots. Theoretical support to the TDDB models is mainly based on the assumption that weak bonds in the dielectric can be broken, or the Cu ions can diffuse out and drift either into the dielectric or along the dielectric/barrier interfaces.^{3–5} The factors, such as Cu chemical-mechanical polishing (CMP), post-CMP annealing, line edge roughness, and fine line effect, which could influence the Cu/ultra-low-k interconnects TDDB lifetime model, have also been reported.^{6,7}

Of equal importance to the TDDB lifetime model is the breakdown mechanism. In recent years, the TDDB behaviors of the ultra-low-k have been studied from aspects of different dielectric materials, process effects, and failure-dominated factors.⁸ Degradation and breakdown of the ultra-low-k dielectrics have been studied by many research groups and a common approach involves the investigation of the conduction mechanism and leakage path in the dielectrics. Yiang investigated the electrical conduction in carbon-doped silicon oxide (SiOC) using a voltage ramp method with electrical conduction in the SiOC over an electric field range of

0 MV/cm to the breakdown field at 300 K.⁹ In his results, the dominant current conduction mechanisms were identified by fitting slopes for various conduction mechanisms at the different ranges of electric field. Atkin studied the charge trapping mechanisms at the ultra-low-k dielectric-silicon interface by using the conductance and capacitance techniques.¹⁰ Trap states close to the interfaces in thin films of porous ultra-low-k dielectrics are expected to affect interfacial barriers with contacts and consequently results in electrical leakage and reliability issues in these materials. Chen reported his observation of the space charge limited current (SCLC) induced by injection of Cu ion into porous ultra-low-k dielectrics.¹¹ It was suggested that the CLC, characterized by the momentary rise and fall of current with time, was found in all Cu interconnects having defective Ta barrier while it was absent in the interconnects with intact barrier.

Direct evidence and clear understanding on the cause and effect of the sources of TDDB failure are still lacking in most of the current investigations. It is well known that the complementary application of Raman and Fourier transform infrared (FTIR) vibrational spectroscopy is one of the most common characterization tools and methodology for low-k and ultra-low-k material analyses and characterization.^{12–16} Due to the challenges of capturing Raman and FTIR spectrum on the patterned wafers, as far as we know, there has been no publication on Raman and FTIR analyses for TDDB failure. Recent progress of the complementary Raman and FTIR vibrational spectroscopy on nanometer-scaled structures on patterned wafers allows for the application of these techniques for TDDB analysis.¹⁷ In this letter, we will present our investigation on the application of complementary vibrational spectroscopy, on alternating interconnect nanostructures and the evidence of dielectric's degradation of the ultra-low-k materials. This investigation provides a methodology to study

^{a)}Electronic mail: maggie.huang@globalfoundries.com.

the breakdown mechanism on low- k and ultra-low- k dielectrics during a reliability test. This letter details observations on degradation behavior found in Cu/ultra-low- k damascene structures and discusses their implication for ultra-low- k technology.

The combination of vibrational spectroscopy of *in-situ* micro-FTIR with micro-Raman was carried out to characterize the ultra-low- k dielectric degradation in TDDB tests. The experiments were conducted on the planar comb capacitor structures consisting of 300 Cu lines with a length of $40\ \mu\text{m}$. These test structures were made using standard dual-damascene Cu interconnect process. The ultra-low- k material used in this study was a porous plasma-enhanced chemical vapor deposition (PECVD) SiCOH film fabricated with the pore volume close to 20%, pore size of about 2 nm, and $k \sim 2.7$. In the Cu/ultra-low- k integration process, 10 nm Ta/TaN barrier bi-layer and 50 nm SiN capping layer were formed.

In order to investigate the degradation process before the structure is destroyed by TDDB tests, all measurements were performed at room temperature under an electrical field ranging from 1.3 to 2.6 MV/cm. The Cu line trench has a sloped profile with a top Cu line-to-line spacing of 50 nm and a bottom line-to-line spacing of 70 nm. The local field at the upper interface is hence higher than the local field at the lower interface by at least 1.4 times. The calculation of applied electric field was based on the smaller line-to-line spacing of 50 nm. Computer-controlled Keithley 4200 semiconductor parameter analyzer was used to stress and then measure the current at selected intervals. During the TDDB tests, *in-situ* FTIR spectra were acquired on the whole area of the comb capacitor structures. The FTIR spectra were recorded using reflection mode on a Nicolet 6700 Analytical FTIR spectrometer where the spectrometer was coupled with a Nicolet continuum infrared microscope. MCT/A detector and KBr beam splitter, with a spectra resolution of $4\ \text{cm}^{-1}$, were used for mid-IR ($700\text{--}4000\ \text{cm}^{-1}$) data collection. On the Raman setup, the equipment has a 325 nm air-cooled helium-cadmium CW laser as excitation source and the spectra were measured by JY Horiba T64000 spectrometer. The Raman spectra were captured on the comb capacitor structures before and after the TDDB tests. The “duoscan” capture mode was used in order to avoid UV laser thermal effect on the ultra-low- k film. For the FTIR and Raman spectroscopes, the spatial resolutions were $15\ \mu\text{m}$ and $0.5\ \mu\text{m}$, respectively. At the end of the experiments, transmission electron microscopy (TEM) and energy-dispersive X-ray spectroscopy (EDX) analyses were carried out at the cross section of the Cu line comb structure. The TEM sample was milled and thinned by focused ion beam (FIB) under a beam voltage of 30 keV and a beam current of 80 pA. The prepared lamella was *in-situ* lifted in Helio 450 FIB and then examined using FEI Titan TEM at 200 keV.

Figure 1 shows the typical curve of leakage current versus stress time at the early stage of the TDDB test on the comb capacitor structures. All samples were found to follow the general conduction behavior of the ultra-low- k dielectric, that is, upon the application of the electric field, the current flow was initially high, but decayed exponentially until it reached the saturation level, indicated in the first stress period of AB. The quick initial current decrease is believed to

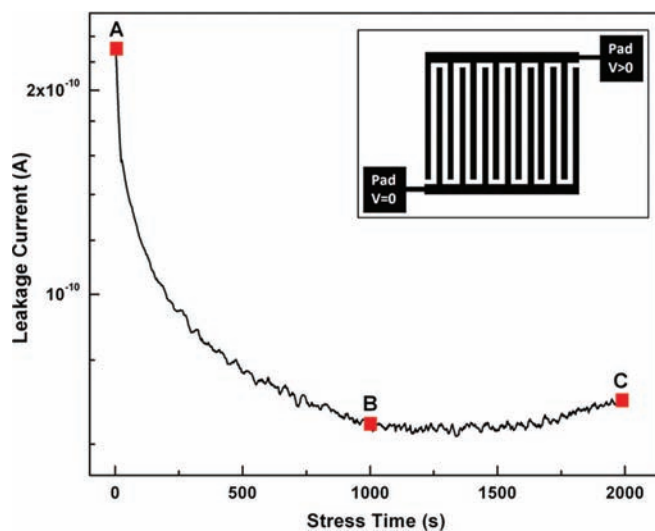


FIG. 1. A plot showing the leakage current as a function of time in Cu/ultra-low- k comb structure. The inset shows the top-down schematics of the comb structure used in the study.

be caused by electron trapping, which thickened the electron tunneling barrier from the cathode into dielectric conduction band. Generally, this conduction mechanism of dielectric is independent of extrinsic factors, such as out-diffusion of Cu ions. However, for the increasing current with increased stressing time, during the second stress period of BC, the dependence of leakage on Cu diffusion is still debated in the published researches.

Figure 2 is the result of *in-situ* FTIR spectra captured on the comb capacitor structure during TDDB test. It shows the chemical bonding evolution in ultra-low- k dielectric from the stress status A to C as indicated in Fig. 1. On the original sample at status A, it can clearly show the ultra-low- k chemical bondings including the network Si-O-Si band at $1027\ \text{cm}^{-1}$, the caged Si-O-Si band at $1035\ \text{cm}^{-1}$, the bending mode of Si-CH₃ band at $1250\ \text{cm}^{-1}$, the Si-H band at $2300\ \text{cm}^{-1}$ and the C-H group bands consisting of the symmetric and asymmetric stretching modes of C-H₃ band at

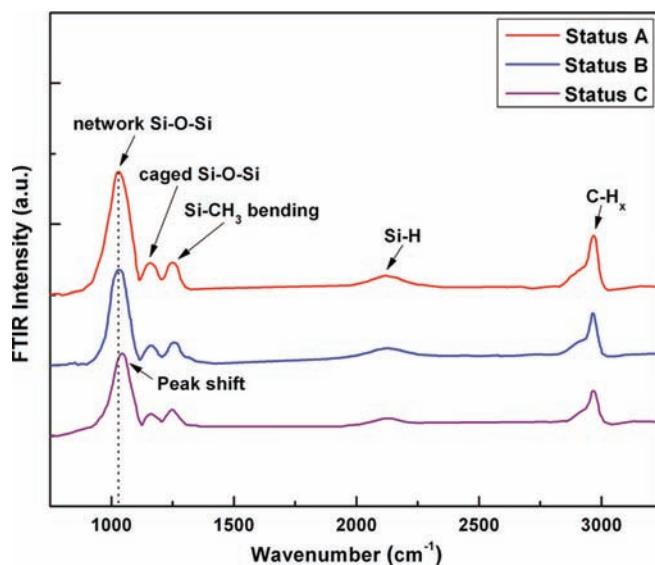


FIG. 2. *In-situ* FTIR spectroscopy on the Cu/ultra-low- k comb structure at different stress status.

2880 cm^{-1} and 2970 cm^{-1} , as well as the symmetric and asymmetric stretching modes of C-H₂ band at 2860 cm^{-1} and 2920 cm^{-1} . After the ultra-low-k dielectric experienced the initial period of leakage decay to a saturation level at status B, its chemical bonding intensity decreased, indicating an occurrence of intrinsic degradation in ultra-low-k dielectric since no extrinsic factors were introduced in this stress period. The result suggests that the injected electrons from cathode have enough energy to break the chemical bonding of ultra-low-k dielectric and the degradation is more severe for the network Si-O-Si bands at 1027 cm^{-1} . When the leakage begins to increase after continued stress (status C), the intensities of chemical bondings of ultra-low-k decrease further. Additionally, a peak shift towards the higher wave frequency vibration is observed for the Si-O-Si network band. It is a combination of effects from both stress and strain on the ultra low-k dielectric. The formation of strain is due to an additional force on the ultra-low-k bonding breakage from bigger size species (compared to electrons) such as metal ions, injected from the anode. The metal ions migration is expected to have caused an increase in the leakage current in the dielectric.

Raman measurement was carried out after the TDDB test for verification of degradation in the ultra low-k structure. Figure 3 shows the Raman spectra captured on the comb capacitor structure before and after stress. The chemical bondings include Si-O-Si symmetric stretch band at 470 cm^{-1} , Si-O-Si asymmetric stretch band at 940 cm^{-1} , Si(CH)_x stretch bands around 780 cm^{-1} , Si-H band at 2170 cm^{-1} , C-H₃ symmetric stretch band at 2920 cm^{-1} , and C-H₃ asymmetric stretch band at 2960 cm^{-1} . Compared to the original sample, all the ultra-low-k bands (especially for the Si-O-Si stretch bands) are obviously degraded after stress. More importantly, a shift towards the lower wave frequency for the asymmetric stretch band of Si-O-Si is observed. This left band shift in the Raman spectra is generally caused by strain, confirming that band damage has occurred in the dielectric during and after the TDDB test.

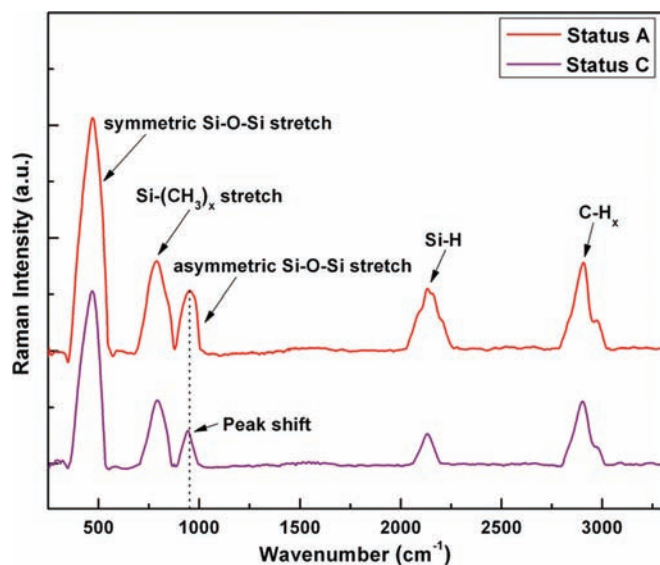


FIG. 3. Raman spectroscopy on the Cu/ultra-low-k comb structure at different stress status.

In order to have a clear understanding of the effect of the leakage current on the ultra-low-k dielectric degradation in TDDB test, high resolution TEM and EDX were used to investigate the possible damage information within ultra-low-k dielectric. Figure 4(a) shows the cross-section image of the comb structure before the application of stress and no abnormality is observed in the original sample. However, Fig. 4(b) shows a severe degradation in ultra-low-k of the comb structure at the stress status C indicated in Fig. 1. It is seen that Ta/TaN barrier bi-layer was decomposed and only a weakened Ta layer was left to cover the Cu lines. EDX line scans along the interface of Cu/Ta/TaN/SiCOH at the anode for both two samples were conducted. Figures 4(c) and 4(d) illustrate that there was no Cu diffusion out of Ta/TaN bilayer in both positions. Comparing with the position shown in the original sample, the Ta/TaN liner peak maximum is much reduced and the width is increased, which confirms that the Ta ions out-migration occurs during TDDB test, but the Ta/TaN bi-layer is sufficient to stop Cu out-diffusion in this condition. This explains the result that the strain measured in vibrational spectra was induced by out-diffused metal ions, which resulted in more damage in ultra-low-k dielectric, manifested by increased leakage current. When the Ta ions drifted into ultra-low-k dielectric, it occurred at a location that was a distance away beneath the capping layer, as shown in Fig. 4(b). This is because the capping layer had a stronger dielectric strength than the ultra-low-k so that the capping layer could push the out-migrating Ta ions into the ultra-low-k volume. Meanwhile, the ultra-low-k dielectric was degraded due to the effect of the electrical field. As a result, migrating Ta ions preferred the path along the weakened ultra-low-k dielectric. The Ta ions diffusion inside ultra-low-k dielectric shows a non-uniform distribution due to the gradient local electrical field formed between Cu lines from upper to lower interface of dielectric and barrier and

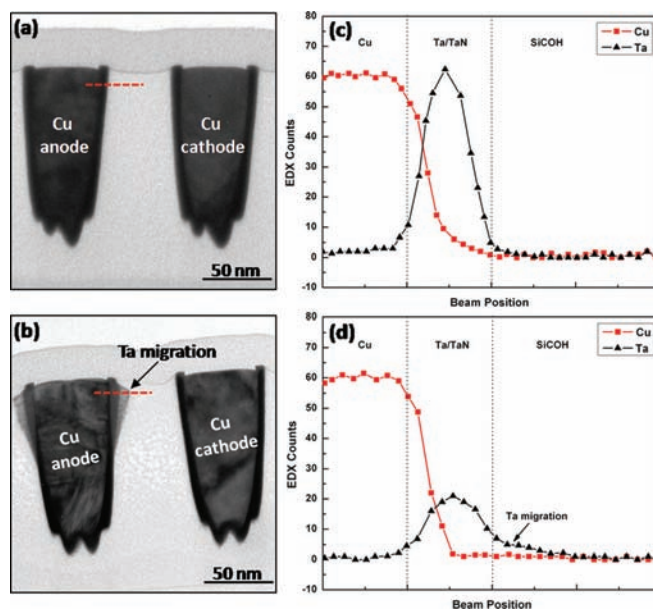


FIG. 4. TEM cross-section images of the Cu/ultra-low-k comb structure for the original sample before stress (a) and the sample with a certain time of stress with leakage current (b). EDX line profile of the Ta migration along the interface of Cu/Ta/TaN/SiCOH before stress (c) and after stress (d), respectively.

capping layer. The highest local electrical field is formed at the upper interface with the smallest Cu line-to-line spacing. Ta ions diffusion reduced the dielectric gap between Cu lines and thus enhanced the local electrical field, which resulted in an acceleration of ultra-low-k degradation to breakdown.

In conclusion, we observed the ultra-low-k dielectric degradation in TDDDB test by the complementary application of Raman and FTIR vibrational spectroscopy. It was found that the intrinsic degradation of the ultra-low-k dielectric would first occur under the applied electrical field, Ta ions would then migrate into ultra-low-k along the weakened interface of Cu/Ta/TaN/SiCOH, causing a more severe damage to the ultra-low-k dielectric. The Ta ions inside the ultra-low-k induced an increased local electrical field between Cu electrodes and thus accelerated the ultra-low-k degradation to final breakdown. In our investigation on the Cu/Ta/TaN/SiCOH structures, no out-diffusion of Cu ions was observed.

We would like to thank the Failure Analysis Lab in Globalfoundries for providing the excellent TEM support, research staff from Nanyang Technological University for the valuable advice and guidance on the experiment, V. Larat from Horiba scientific, and K. C. Ho from Thermo Fisher scientific for the expert discussions and technical assistance on Raman and FTIR experiments.

- ¹International Technology Roadmap for Semiconductors: 2011 Update, page 35.
- ²G. S. Haase, E. T. Ogawa, and J. W. McPherson, *J. Appl. Phys.* **98**, 034503 (2005).
- ³K. Maex, M. R. Baklanov, D. Shamiryan, F. Iacopi, S. H. Brongersma, and Z. S. Yanovitskaya, *J. Appl. Phys.* **93**, 8793 (2003).
- ⁴W. Volksen, R. D. Miller, and G. Dubois, *Chem. Rev.* **110**, 56 (2010).
- ⁵M. R. Baklanov and K. Maex, *Phil. Trans. R. Soc. A* **364**, 201 (2006).
- ⁶M. Stucchi, P. J. Roussel, Z. Tokei, S. Demuyne, and G. Groeseneken, *IEEE Trans. Device Mater. Reliab.* **11**, 278 (2011).
- ⁷J. Noguchi, *IEEE Trans. Electron Devices* **52**, 1743 (2005).
- ⁸F. Chen, O. Bravo, D. Harmon, M. Shinosky, and J. Aitken, *Microelectron. Reliab.* **48**, 1375 (2008).
- ⁹K. Y. Yiang, W. J. Yoo, Q. Guo, and A. Krishnamoorthy, *Appl. Phys. Lett.* **83**, 524 (2003).
- ¹⁰J. M. Atkin, E. Cartier, T. M. Shaw, R. B. Laibowitz, and T. F. Heinz, *Appl. Phys. Lett.* **93**, 122902 (2008).
- ¹¹L. S. Chen, W. H. Bang, Y. J. Park, E. T. Ryan, S. King, and C. U. Kim, *Appl. Phys. Lett.* **96**, 091903 (2010).
- ¹²C. Cartereta and A. Labrosseb, *J. Raman Spectrosc.* **41**, 996 (2010).
- ¹³N. J. Trujillo, Q. Wu, and K. K. Gleason, *Adv. Funct. Mater.* **20**, 607 (2010).
- ¹⁴A. Grill and D. A. Neumayer, *J. Appl. Phys.* **94**, 6697 (2003).
- ¹⁵J. Bao, H. Shi, J. Liu, H. Huang, P. S. Ho, M. D. Goodner, M. Moinpour, and G. M. Kloster, *J. Vac. Sci. Technol. B* **26**, 219 (2008).
- ¹⁶H. L. Shi, J. Bao, R. S. Smith, H. Huang, J. Liu, P. S. Ho, M. L. Mcswiney, M. Moinpour, and G. M. Kloster, *Appl. Phys. Lett.* **93**, 192909 (2008).
- ¹⁷J. C. K. Lam, M. Y. M. Huang, H. Tan, Z. Q. Mo, Z. H. Mai, C. P. Wong, H. D. Sun, and Z. X. Shen, *J. Vac. Sci. Technol. A* **29**, 051513 (2011).